

Estimate of the debris-flow entrainment using field and topographical data

Clàudia Abancó · Marcel Hürlimann

Received: 6 June 2013 / Accepted: 26 October 2013 / Published online: 6 November 2013
© Springer Science+Business Media Dordrecht 2013

Abstract The entrainment of material is a common process in debris-flow behaviour and can strongly increase its total volume. However, due to the complex nature of the process, the exact mechanisms of entrainment have not yet been solved. We analysed geomorphological and topographical data collected in 110 reaches of 17 granular debris flows occurred in the Pyrenees and the European Alps. Four governing factors (sediment availability, channel-bed slope, channel cross section shape and upstream-contributing area) were selected and defined for all the 110 reaches. One dataset of the resulting database was used to develop two models to estimate the erosion rates based on the governing factors: a formula derived from multiple linear regression (MLR) analysis and a decision tree (DT) obtained from J48 algorithm. The models obtained using these learning techniques were validated in another independent dataset. In this validation set, the DT model revealed better results. The models were also implemented in a torrent (test set), where the total debris-flow volume was known and two empirical methods (available in literature) were applied. This test revealed that both MLR and DT predict more accurately the final volume of the event than the empirical equations for volume prediction. Finally, a general DT was proposed, which includes three governing factors: sediment availability, channel-bed slope and channel cross section shape. This DT may be applied to other regions after adapting it regarding site-specific characteristics.

Keywords Debris flow · Entrainment · Field · Topographical

1 Introduction

Debris flows are fast mass movements, formed by a mix of water and solid materials, which mostly occur in steep torrents. They represent a major risk to human settlements and

C. Abancó (✉) · M. Hürlimann
Department of Geotechnical Engineering and Geo-Sciences, Technical University of Catalonia
BARCELONATECH, C/Jordi Girona, 1-3 (D2), 08034 Barcelona, Spain
e-mail: claudia.abanco@upc.edu

infrastructures in mountainous areas. The basal entrainment of channel-bed material is a common feature of debris flows. Debris-flow torrents often consist of colluvium and other types of coarse sediment, which can be partially or totally incorporated into the flowing mass (Pierson and Scott 1985; Hungr et al. 2005). The entrainment of loose and unconsolidated material along the flow path affects fundamental parameters used for debris-flow hazard assessment, since it directly influences the volume and flow dynamics (Mangeny et al. 2010; Iverson et al. 2011). In debris-flow hazard assessment, the erosion rate is a common term to describe the amount of material incorporated into the flowing mass per unit of length (Hungr et al. 1984).

The total volume of the debris flow can be considerably enlarged due to the entrainment (Hungr et al. 2005; Guthrie et al. 2009; Berger et al. 2011). Studies on individual events with remarkable erosion are available in literature (Scheidl et al. 2008; Theule et al. 2012), as well as in some regional datasets on entrainment (Fannin and Rollerson 1993; Hungr et al. 2005; Gertsch 2009). These data revealed that the material entrained along the flow path can reach a high percentage (up to 90 %) of the total volume of the events. For this reason, it is a key question to predict the potential volume that can be entrained along the flow path.

The theoretical basis to evaluate the entrainment and to predict erosion rates has strongly improved (e.g. Iverson 2012). However, the practical application of this concept has not yet been solved. Most of the approaches that determine the volume of debris flows are based on estimations of the entire volume of the event, while only few specifically incorporate the effect of entrainment. The approaches to estimate the event volume could be divided into two principal groups: (1) empirical methods and (2) physically based methods.

The empirical methods can be separated into two groups: simple equations and field or geomorphological methods. The simple equations are usually based on few terrain parameters. Many authors have developed this type of equations, such as VanDine (1985), Takei (1984), Zeller (1985), Franzi and Bianco (2001), Marchi and D'agostino (2004), Dong et al. (2009) among others. These approaches incorporated the catchment area and correlated it to the volume of the debris flow by means of expressions such as $V = kA^b$. Other authors included one or two additional parameters such as the torrent slope and an adimensional factor of torrentiality (Kronfeller-Kraus 1985), the torrent slope and a geological index (D'Agostino 1996) or the run-out distance instead of the catchment area (Rickenmann 1995). These approaches are defined to be applied at the entire torrent scale, without considering local changes in the torrent characteristics and erosion rates. The field or geomorphological methods consist of estimations of erosion rates based on the morphology of the torrent or its specific reaches. These methods consist of geomorphological descriptions of the torrents to identify and to quantify in some occasions, the potential sediment sources (Fannin and Rollerson 1993; Hungr et al. 1984; Spreafico et al. 1999; Fannin and Wise 2001).

The physically based methods include both static and hydrodynamic approaches and describe the mechanics of the channel-bed scouring and lateral bank failures. Many of these approaches have been derived from laboratory observations (Egashira et al. 2001; Rickenmann et al. 2003; Papa et al. 2004) or a large outdoor flume (Iverson et al. 2011). Some numerical models have included physical approaches into the codes (e.g. McDougall and Hungr 2004; Crosta et al. 2009; Medina et al. 2008), while others use algorithms derived from empirical approaches (Degetto et al. 2011) or simply exclude the effect of this mechanism (Denlinger and Iverson 2001).

Besides the uncertainties of defining the mechanism of the entrainment itself, the difficulties start with the ambiguities in the definition of the governing factors of the process. The empirical methods have typically incorporated terrain factors, which can be assessed by simple topographical calculations or by field campaigns. However, the influence of each factor in the erosion rate has only been studied by few authors (Chen et al. 2005; Hungr et al. 2005; Guthrie et al. 2009; Mangeney 2011). The results show a large scattering, which suggests that the mechanisms governing the entrainment are complex and that different factors influenced the entrained volume.

The main goals of this publication are threefold: first, we present and analyse the database collected at recent debris flows in order to determine the characteristics of the entrainment and the governing factors. Second, we propose and compare two approaches related to learning techniques to predict the amount of material that can be entrained from the channel bed along the flow path. Third, we present a simple and general approach to estimate the entrainment, which should be applicable without extensive field work.

2 Study regions and database

Entrainment data on 17 debris flows were collected in this study. All the debris flows are granular-type (Coussot and Meunier 1996). Data collection was carried out during field surveys and was complemented using a geographic information system (GIS). The surveyed debris-flow torrents are located in the Pyrenees and the European Alps (Fig. 1).

The central-eastern sector of the Pyrenean mountain range limits the Spanish autonomy of Catalonia from France and also includes the Principality of Andorra. The highest peaks show altitudes slightly over 3,000 m a.s.l. and are located in the central Pyrenees. From a geological point of view, the bedrock of the Axial Pyrenees mainly consists of a basement of igneous and metamorphic Paleozoic rocks folded, intruded and metamorphosed during the Hercynian orogeny (Muñoz 1992). The southern outer part of the range, coinciding with the Pre-Pyrenees, is composed of sedimentary sequences mostly of Mesozoic ages. The superficial deposits predominantly consist of colluvium. The sites (13) are located in periglacial areas, where weathering, erosion and hill slope processes are the principal agents for sediment supply in the channels. Most catchments are weathering-limited or supply-limited systems after the classification of Bovis and Jakob (1999). The debris-flow activity in the Pyrenees is lower than the activity of other mountain ranges; however, recent studies prove that in some catchments, it is much higher than expected (Hürlimann et al. 2013). The events took place during a short period of time and high-intensity rainfall episodes related to convective summer storms.

Four debris flows occurring in the European Alps (A) were analysed (Table 1). The European Alps cross Western Europe along ~1,200 km and include many peaks over 4,000 m a.s.l. (the maximum elevation is 4,810 m). In short, they comprise different nappes (Pennine, Helvetic and Austroalpine) of sedimentary to metamorphic rocks and a crystalline basement. The three Swiss events are located in areas where the Helvetic nappe, and partially the crystalline basement crop out, while the Austrian event is situated in the National Park ‘Gesäuse’ within the northern limestone Alps. All the sites are located in periglacial areas, affected by high-mountain morphologic processes and by a minor importance of the erosional activity of the torrents. All events occurred during the summer and were triggered by convective storms with high rainfall intensities.

The events selected for this study are constituted by reaches with a wide range of erosion rates. Therefore, the database includes a large variety of governing factors and



Fig. 1 Location of the surveyed debris-flow torrents in the Pyrenees (a) and the European Alps (b). All the torrents used in this study (training set, validation set and test set) are shown

erosion. The database contains events initiated both by a landslide and by run-off, and the final volumes range from hundreds to tens of thousands of cubic metres (Table 1). These final volumes of the events were estimated from our field data or taken from technical reports (Marquis 2006, 2008; Pinyol 2008; Oller and Pinyol 2009). The field surveys were mostly carried out days or weeks after the events. Only in a few cases, the data collection took place after a longer period of time.

The estimates of erosion rates were based on the field observations of erosion evidence and reconstruction of the sediment disposition before the event (Fig. 2). For some reaches, an airborne LIDAR digital elevation model (of the pre-event situation) was available. For the other reaches, where a digital elevation model was not available, the reconstruction of both channel bed and banks was done based on expert criteria. The morphologic comparison between parts of the cross section that were not affected by the event (above the maximum flow depth) and the parts where the entrainment occurred was a key point for the reconstruction. The estimated erosion rates include changes on the cross section (including channel bed and banks) but not lateral failures that can occur in the channel-adjacent slopes. Finally, for each event, two types of input data were incorporated into the database: (1) field observations and (2) morphometric data derived from digital elevation models (DEM) with pixel size ranging from 1 to 5 m.

Table 1 Main characteristics of the debris flows included in the database

Name	Date of the event (mm/yyyy)	Estimated V (m ³)	Catchment area (km ²)	Averaged erosion rate (m ³ /m)	Mean channel slope (°)	Number of reaches	Initiation mechanism	Area of study
Varradòs	11/2011	~ 1,500	0.2	1.5	35	7	R	AP
Sant Nicolau	05/2008	1,800	0.7	0.87	19	4	L	AP
Llebreia	~ 2000	2,350	0.03	0.56	22.5	4	L	AP
Port Ainé	09/2008	26,000	5.6	2.12	15	8	R	AP
Reguerals	08/2009	1,500	4.4	1.12	21.5	2	R	AP
Riu Runer	08/2008	14,000	8.2	1.85	14	13	R	AP
Fontanals	08/2008	1,500	0.4	1.37	31	6	R	AP
Setcases	08/2010	~ 800	0.9	0.25	27	2	R	AP
Montaup	07/2010	900	5.3	0.55	17	10	R	AP
Vilacireres	11/1982	11,000	0.2	3	22.5	1	L	PP
Ensija	2006	1,500	0.7	2.12	19.2	6	R	PP
Tagast	11/1982	5,000	0.5	2.83	12.5	3	L	PP
Torrent de la Molina	~ 2011	12,000–16,000	0.8	3.74	17.1	18	L	AP
Torrent des Glariers	07/2006	4,000–5,000	1.3	1.37	33.5	4	R	EA
Torrent Sec	06/2008	20,000	1.4	1.89	33	10	R	EA
Schlipfenbach	08/2000	5,000	1.4	2.1	45	7	R	EA
Gesäuse	2009	1,200	0.01	2.8	32.5	5	R	EA

R run-off, L landslide, AP axial pyrenees, PP pre-pyrenees, EA European Alps

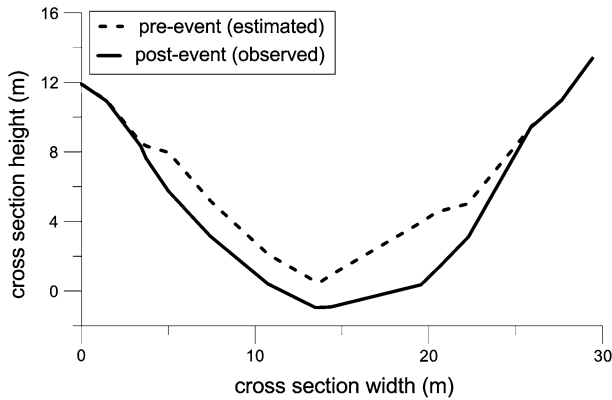


Fig. 2 Sketch of the cross section of a channel reach indicating how erosion rate was estimated

3 Methods

3.1 Governing factors

The 17 torrents were divided into reaches according to similar geomorphological features and erosion rates. Thus, the final database contains 110 reaches of debris-flow torrents. The length of the reaches ranges from tens of metres to more than one thousand metres.

In every reach, different terrain features were determined, herein called governing factors. Four governing factors were selected for each reach i : (1) reach-averaged slope (S_i), (2) sediment availability (SA_i), (3) cross section shape (CS_i), and (4) upstream-contributing area (UCA_i). These factors can be divided into two groups depending on the collecting method: (1) three field factors (S_i , SA_i , CS_i) and (2) one topographical factor (UCA_i). The factors can also be distinguished between numerical (S_i , UCA_i) and categorical ones (SA_i , CS_i). The choice of these factors was based on: (1) the simplicity of their collection, (2) field observations that prove their influence on the entrainment process (regarding the field governing factors) and (3) experiences obtained from previous studies (e.g. Hungr et al. 2005).

3.1.1 Reach-averaged slope

The reach-averaged slope of a specific reach (S_i) is a numerical factor measured in degrees. In our work, the slope of the reaches was measured in the field using a standard clinometer: one single measurement for short reaches (few tens of metres) and several ones for longer reaches, which are then averaged to obtain the reach-averaged slope. The slope of the longest reaches was compared to the one provided by the DEM. This comparison showed that the values obtained from both methods were similar.

Some authors studied the relation between the erosion rate and the slope of the torrent reaches or of individual points in the channel. In some cases, the relation shows that the slope increases, as the entrainment rate enlarges (Rickenmann and Zimmermann 1993; Guthrie et al. 2009). This result would stress the importance of the slope on the entrainment process. In other circumstances, however, it has been observed that there is a feedback effect, which means that the entrainment is higher at low slopes. The justification of this effect was the increasing flow concentration or peak discharge with longer distances, which is normally associated with a slope decrease (Breien et al. 2008). Other studies contradict

these two cases indicating that there is no clear trend, as the erosion rate is completely related to the availability of sediment in the reach (Hungre et al. 1984; Marchi et al. 2009).

3.1.2 Sediment availability

The sediment availability in reach i (SA_i) is a categorical factor. According to our observations in the field, it is one of the most influencing factors in the entrainment during a debris flow. In some torrents, reaches may show unlimited sediment (here called “unlimited” reaches). Thus, the erosion produced is totally conditioned by other factors. While in other reaches, the lack of sediment limits the entrainment. The importance of sediment availability on the entrainment has been demonstrated in several occasions by other authors (Bovis and Jakob 1999; Jakob et al. 2005).

In this work, five classes were described depending on how much material is available in the torrent reach. The distinction of classes is based on the percentage of the cross section that is covered by a certain thickness of sediment (Table 2).

3.1.3 Cross section shape

The reach cross section shape (CS_i) is a categorical factor. Although the cross section shape is not considered in previous works as a governing factor for the entrainment process, we incorporate this aspect, because it illustrates the degree of incision of the channel before the event and thus affects the flow dynamics.

In order to determine the shape of the cross section, the concept proposed by Gabet and Bookter (2008), who studied the shape of some gullies in south-west Montana (USA) based on a shape index, was adapted. The width was established at a certain height above the thalweg before the event, being the relevant dimension to describe the reach incision. The height was chosen with expert criteria, as an estimate of the flow depth that achieved the debris flow in the specific reach. In order to simplify field work and subsequent data analysis, the cross section shape factor was divided into the three classes “wide”, “moderately incised” and “incised” instead of using the exact width (Table 3). The class limits were established based on the observation during the field surveys in the torrents.

3.1.4 Upstream-contributing area

The reach’s upstream-contributing area (UCA_i) is a numerical factor that can easily be determined in GIS. It is calculated as the sum of map units (pixels) that drain water and other substances to the lowest point of a reach. The sum value of the pixels is obtained by means of the flow accumulation tool found in ArcGIS® (ESRI 2005), using a DEM.

The upstream-contributing area is applied in this work to illustrate the differences of discharge and sediment transport between reaches. For example, a debris flow can initiate into a similar concentration as a hyper concentrated flow in the upper reaches of the torrent (smaller upstream-contributing area) and be totally developed to a mature debris flow lower at the fan apex, where the upstream-contributing areas are larger.

The general patterns were analysed for each governing factor (S_i , CS_i , SA_i , UCA_i) and for the target variable (e_i). The analysis was performed by means of histograms and correlations between variables for the entire database of 110 reaches.

Table 2 Sediment availability classes


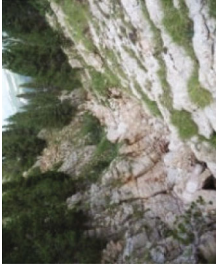
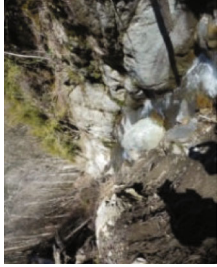
Class	Image	% of bedrock at cross section	% of colluvium at cross section	Thickness of colluvium layer (m)
Complete limitation (CL)		> ~90	< ~10	< ~0.5
High limitation (HL)		> ~75	< ~25	< ~1
Medium limitation (ML)		~50	~50	~1

Table 2 continued



Class	Image	% of bedrock at cross section	% of colluvium at cross section	Thickness of colluvium layer (m)
Low limitation (LL)		< ~25	> ~75	> ~1
No limitation (NL)		< ~10	> ~90	> ~1

Table 3 Cross section shape classes

Class	Wide	Moderately incised	Incised
Image			
Characteristics	$W > 5H$	$2H < W \leq 5H$	$W \leq 2H$
W width, H height			

3.2 Multiple linear regression

The multiple linear regression (MLR) is a learning technique, whose intent is to find out the best linear relationship between the erosion rate in a particular reach (e_i) and the governing factors using the following expression:

$$e_i = a_1S_i + a_2SA_i + a_3CS_i + a_4UCA_i + b. \quad (1)$$

The coefficients a_1 , a_2 , a_3 , a_4 and b are determined by minimizing the sum of the squared errors originated by the approximation of the erosion rate in every reach of the dataset. A numerical value was attributed to the categorical factors (CS and SA). For example: a “wide cross section shape” is represented by 1, a “medium cross section shape” by 2 and an “incised cross section shape” by 3. The same was done with the SA, although numbers range from 1 (complete limitation of sediment) to 5 (no limitation of sediment). Therefore, the resulting erosion rate is a numerical value.

Previously to the application of the MLR to the training set (93 reaches), the distribution of the variables was taken into account. If some of the variables in the dataset present a distribution far from normal, it is common to perform a transformation of the dataset. By transforming the data, a normal distribution of the values of a certain variable was achieved (Gartner et al. 2008).

3.3 Decision tree

Decision trees are a family of learning techniques that have been used by several authors in the field of natural hazards (Wan and Chiang Lei 2009; Chevalier et al. 2013). DTs allow the use of categorical values directly. They are based on two main elements: nodes and leaves. At each node, an attribute (governing factors) is tested. The procedure consists in comparing the attribute with a certain value (in numerical attributes) or choosing a specific category (in categorical attributes). At a certain level of the tree, a leaf is reached, which means that a final category of the target variable is achieved.

To create the DT, we used the data mining-software WEKA (Hall et al. 2009). Data mining is the process of discovering patterns, sometimes hidden, in a database (Fayyad et al. 1996). WEKA incorporates a total of 77 algorithms of learning techniques, from which 16 are DTs. Many of them were tested, achieving the best results in the J48 DT. The algorithms of the DTs are not discussed herein but are explained in Breiman et al. (1984). That is why herein only results from DT J48 are presented. We selected a 10-fold cross validation method to optimize the tree.

The DT learning process can present problems, if the target variable is not equally distributed. For this reason, the cost matrixes are a common strategy in the definition of DTs in imbalanced datasets (Witten et al. 2011). They are implemented as a metaclassifier during the learning process to force that all of the target classes appear in the tree. The matrix components provide a cost value for each class that would be misclassified into another class. Another problem in the definition of DTs is the overfitting, which creates extremely complex trees. One of the strategies to avoid overfitting is pruning (Witten et al. 2011). The pruning parameters are set in the classifier and affect the size of the tree and its complexity.

3.4 Validation and test of models

The evaluation of the success of the models was structured in two parts. Firstly, the two models were assessed by comparing which of them fits better with the validation set (ten reaches, representative for the whole dataset and randomly selected). Secondly, both

models were tested in a torrent where the final volume of the event and the erosion rates of the reaches are known (test set, seven reaches). In this part, a comparison between the models (MLR and DT) and two existing empirical formulae was carried out.

The first part (validation) consists in evaluating the success of the models obtained by the learning techniques. The success of different predicting models is usually based on the receiver-operating characteristics, also called ROC analysis (Fawcett 2006). Common parameters used for ROC analysis are the true positive rate (TPR) and the false positive rate (FPR). Typically, the values of the TPR and FPR are plotted in a ROC graph. Then, the values are compared to the diagonal line ($y = x$), in case the predicted variable has two classes.

Since our predicted variable (the erosion rate) has more than two classes, the ROC analysis and Precision–Recall curves become more complicated. Thus, the ROC space is n -dimensional being n the number of classes of the variable and a visualization in the bi-dimensional ROC space is impossible. Therefore, we calculated the F -measure parameter to test the performance of the models for each class of entrainment. This F -measure parameter can be expressed by:

$$F = \frac{2 \cdot \text{precision} \cdot \text{recall}}{(\text{precision} + \text{recall})}. \quad (2)$$

This expression combines the precision (true positives over total positives) and the recall (true positives over the sum of true positives and false negatives) of each class. This is the weighted harmonic mean of these two parameters (Hripcsak and Rothschild 2005). The comparison of the F -measure for each entrainment class illustrates whether a model is especially advantageous for a certain entrainment class. This could be meaningful in case the class is especially representative in the database.

The second part (test) consists in applying the models to a torrent from the database that was used neither in the training nor in the validation processes. The Schipfenbach torrent (Fig 1b; Table 1), which includes seven reaches, was selected as test set because of its variability in the governing factors and the erosion rates. The two learning techniques as well as two simple empirical methods were applied to the Schipfenbach torrent and the final debris-flow volume was calculated for each methodology. The observed total volume of entrainment along the torrent is known from field observation after the event (Hürlimann et al. 2003).

The two selected empirical formulae are one proposed by Rickenmann (1995)

$$\theta_f < 15 \% : V = (6.40\theta_f - 23) L; 15 \% < \theta_f < 40 : V = (110 - 2.5 \theta_f) L, \quad (3)$$

where θ_f is the fan slope in (%), V is the volume of the event and L is the run-out length; and another suggested by D'Agostino (1996)

$$V = 45 A^{0.9} \theta^{1.5} (\text{I.G.}), \quad (4)$$

where θ is the mean slope of the channel; I.G. is a geological index. For the DT, two different volumes were computed taking into account the minimum and maximum values of the erosion rate classes for all the reaches.

4 Results

4.1 Statistical distribution of the governing factors

The database contains a total number of 110 torrent reaches located in the Pyrenees (84) and the European Alps (19). Cumulated frequency graphs of the numerical variables and

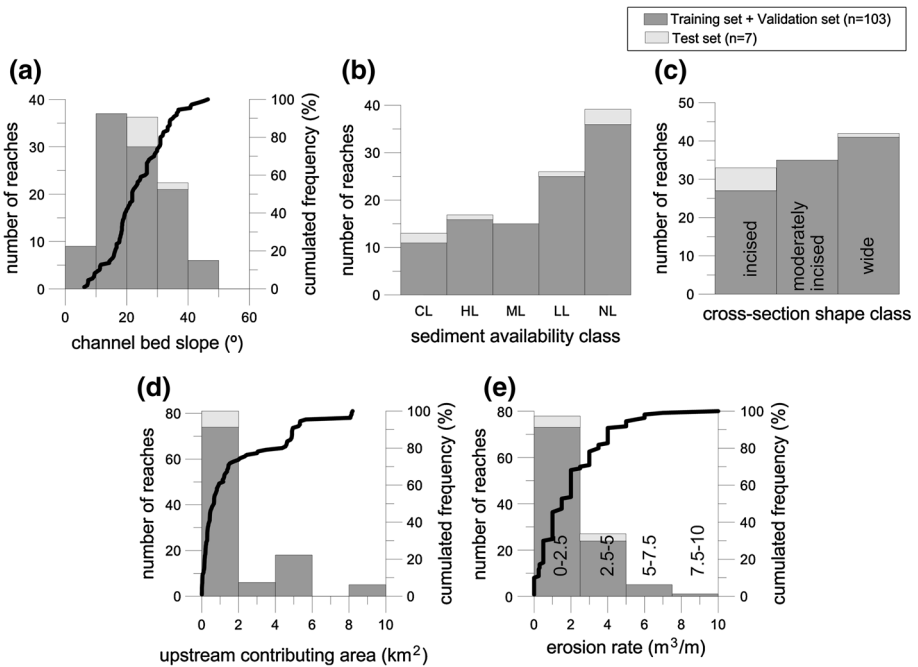


Fig. 3 Histograms of the four governing factors (a, b, c, d) and the erosion rate (e) for the 110 reaches included in the database. The cumulated frequency is shown for the numerical governing factors (a, d) and erosion rate (e). See Table 2 for abbreviations of sediment availability classes

histograms of the four governing factors and the target variable are shown in Fig. 3. In the same Fig. 3, the histograms of the reaches in the test set are also shown.

The histogram of the reach-averaged slope distribution (Fig. 3a) presents a peak in the slope bin of 10°–20°. The most frequent values of the reach-averaged slope are between 10° and 40°, with a mean value of 23° and a standard deviation of 9°. Steeper (>40°) and smoother (<10°) reaches are of low frequency in our dataset, ~6 and ~8 %, respectively. These results fit other published works, in which channel slopes showing erosion range from 18° to 27° (Marchi and D’Agostino 2004), or are higher than 15° (Hungr et al. 2005).

Almost 40 % of the reaches in the database are unlimited (NL) in terms of sediment availability (Fig. 3b) and more than half of the reaches have NL or LL. The cross section shape distribution revealed that incised reaches are the most common ones in our database (Fig. 3c).

The upstream-contributing area of the reaches in the database takes values up to 8.2 km² (Fig. 3d). This value and the total drainage areas (see Table 1) support the hypothesis that a small catchment area is a typical feature for debris-flow occurrence (e.g. Rickenmann and Zimmermann 1993). The histogram shape is strongly skewed to the left, and almost 60 % of the reaches have an upstream-contributing area lower than 1 km².

The erosion rate-cumulated frequency graph shows a gradual increase: sharper for the lower values of the erosion rate and rising slowly for the higher ones (Fig. 3f). The prevalence of low erosion rates (of less than 2.5 m³/m) is also illustrated in the histogram. Although high erosion rates were reported in some reaches, the values reported in our database are similar to the lower classes of erosion rates from similar studies, such as

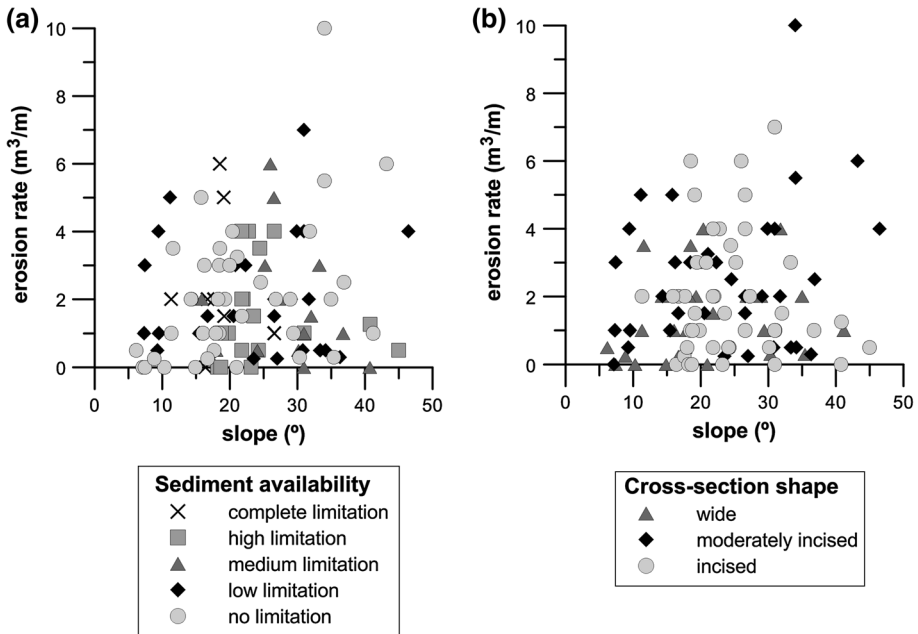


Fig. 4 Relations between slope and erosion rate depending on sediment availability (a) and channel cross section shape (b) for the 92 reaches of the database

Hungry et al. (1984). This can be justified by the exclusion of lateral bank failures and the glacial geological context of Hungry's work.

In order to identify possible relations between governing factor and the target variable or among themselves, many governing factor plots were visualized. In spite of the high dispersion, few general trends could be identified. Regarding the graph that correlates the reach-averaged slope versus erosion rate, a general linear increasing trend between the slope and the erosion rate for the less limited sediment classes (NL and LL) can be observed (Fig. 4a). In the case of more limited sediment classes, the trend cannot be observed. The influence of the cross section shape can be observed in Fig. 4b, where it can hardly be observed that higher erosion rates occur preferably in incised reaches than in moderately incised or wide reaches.

4.2 Multiple linear regression

The histograms of the previous section show that some variables present a distribution far from normal, particularly skewed to one side: upstream area, erosion rate, sediment availability or cross section shape. As mentioned above, a transformation of the values of these variables could help to get better results in the learning process. Only two of these variables are numerical; and therefore, a transformation of the values could be applied to their values: erosion rate and upstream area. We performed two different types of modifications on these variables in order to transform them in normal-distributed variables. We carried out a log-transformation and ln-transformation. Moreover, to ensure the importance of each of the variables in the analysis, we carried out a step-by-step MLR analysis. In each

step, we added a new variable. Therefore, we can ensure that adding variables increases the success of the methodology.

The results of the MLR applied to the original training set (without transformation of area upstream and erosion) and the transformed training sets are shown in Table 4a. Two parameters were chosen to compare the three attempts: the R^2 and the standard error. The models with highest R^2 value and lowest standard error are the ones with best performance. Thus, when the erosion rate and the area upstream are log-transformed, best results are obtained. The purpose of the second part of the analysis was to verify, whether accuracy depends on the quantity of governing factors included in the MLR. The results confirm that the best performance is achieved when using all the parameters (Table 4b).

Therefore, the final equation obtained by the MLR is a first-order polynomial expression of five variables and can be expressed by:

$$\log(e_i + 1) = 0.007 S_i + 0.102 SA_i - 0.066 CS_i + 0.053 \log(UCA_i + 1) - 0.312. \quad (5)$$

4.3 Decision tree

The resulting tree applying the J48 algorithm to the training set is shown in Fig. 5. The predicted erosion rate was divided into four classes with an interval of 2.5 m³/m (the same classes as the ones shown in the histogram in Fig. 3e). The interval of 2.5 m³/m is considered to be a reasonable resolution of an erosion rate class for our database. In addition, such a classification of this parameter supports our goal to propose a simple methodology.

First, a cost matrix was used with the intention to avoid the problems derived from the imbalance of the erosion rate distribution. The cost matrix was defined in order to force that the four classes of the erosion rate appear in the final DT. It was done by means of attributing higher costs to the misclassification of reaches with larger erosion rates (less present in the database). Second, the pruning was set by a confidence factor of 0.25 after several attempts. This confidence factor provided a DT with a maximum of three levels, which was acceptable according to the aim of defining a simple model.

Table 4 Results from MLR analysis. (a) Different attempts with different data transformations. (b) Step-by-step analysis of the different parameters (log-transformed values of upstream-contributing area and erosion rate)

(a)			
Attempt	Training dataset	R^2	SE
1	Data not transformed	0.27	1.61
2	E and UCA log-transformed	0.3	0.22
3	E and UCA ln-transformed	0.3	0.5
(b)			
Step	Governing factors in dataset	R^2	SE
1	SA	0.19	0.23
2	SA and CS	0.25	0.22
3	SA, CS and S	0.3	0.22
4	SA, CS, S and UCA	0.31	0.22

SA sediment availability, CS cross section shape, S slope, UCA upstream-contributing area, E erosion rate, SE standard error

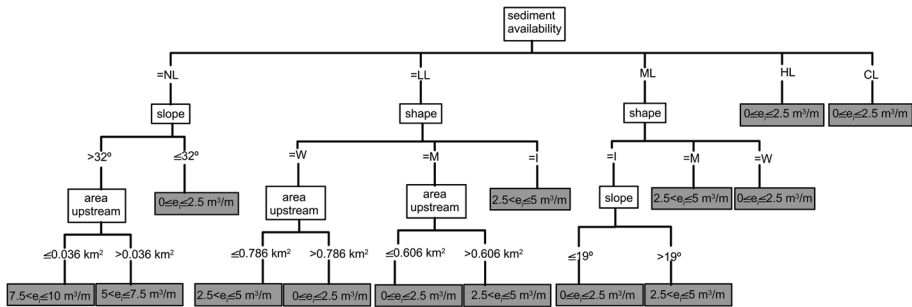


Fig. 5 Decision tree for entrainment estimate using the training set of our database applying the algorithm J48

The first split of the tree refers to the sediment availability, and the branches with fewer availability of sediment (CL and HL) already reach the final leaf. These leafs correspond to the class of the lowest erosion rates. The branches with more sediment available (ML, LL and NL) need one or two additional levels to reach the leaf of the value of the erosion rate.

The cross section shape is the second factor appearing in two of the classes of sediment availability, while the average slope of the reach exists in one. In the following level of the tree, the slope or the upstream-contributing area is located. In general, the dominant class in the DT is the lowest erosion rate class: “ $0 \leq e_i \leq 2.5 \text{ m}^3/\text{m}$ ”, appearing in half of the leafs of the DT. The maximum erosion classes only appear in steep reaches ($<32^\circ$) with unlimited sediment availability.

4.4 Validation and test of models

The validation of the two models was based on the *F*-measure parameter, as mentioned in previous sections. The *F*-measure was calculated for each of the classes of the erosion rate, both in the training set and in the validation set. The values in Table 5 suggest that both techniques show good performance in the lowest class of erosion rate (up to $2.5 \text{ m}^3/\text{m}$) in both training set and test set. This is a reasonable result, as this is the most frequent erosion rate class. However, for the larger erosion rate classes, MLR does not offer good results. Thus, the weighted average of the *F*-measure was calculated to get an overall evaluation. Regarding the weighted average, the DT learning technique showed better results, especially in the training set, but also in the validation set.

The test of the models revealed two main ideas (Fig. 6): first, MLR-estimation and the maximum value estimated by DT coincide very well with the observation, while the minimum value estimated by DT underestimates the volume. Second, the volumes determined by the two empirical relationships strongly overestimate the observed volume by more than one order of magnitude. This result can be attributed to various facts: empirical equations always have a large scatter, and the results can consequently have important errors; the empirical techniques were developed in a specific area, and their application to other regions may generate inaccuracy.

5 New general approach to estimate entrainment

We selected the DT model to propose a new general approach that estimates the entrainment. Empirical formulae may be adequate for a preliminary estimate without time-

Table 5 Values of the *F*-measure parameter for each class of the two models to predict the entrainment in the training and the validation set

Model	Class	Training set		Validation set	
		<i>n</i> (total 93)	<i>F</i> -measure	<i>n</i> (total 10)	<i>F</i> -measure
Multiple linear regression (MLR)	$0 \leq e_i \leq 2.5 \text{ m}^3/\text{m}$	67	0.940	6	0.714
	$2.5 < e_i \leq 5 \text{ m}^3/\text{m}$	17	0.117	3	0
	$5 < e_i \leq 7.5 \text{ m}^3/\text{m}$	8	0	1	0
	$7.5 < e_i \leq 10 \text{ m}^3/\text{m}$	1	0	0	0
	Weighted average	0.632		0.429	
Decision tree (DT)	$0 \leq e_i \leq 2.5 \text{ m}^3/\text{m}$	67	0.917	6	0.857
	$2.5 < e_i \leq 5 \text{ m}^3/\text{m}$	17	0.649	3	0.8
	$5 < e_i \leq 7.5 \text{ m}^3/\text{m}$	8	0.4	1	0
	$7.5 < e_i \leq 10 \text{ m}^3/\text{m}$	1	0.5	0	0
	Weighted average	0.819		0.754	

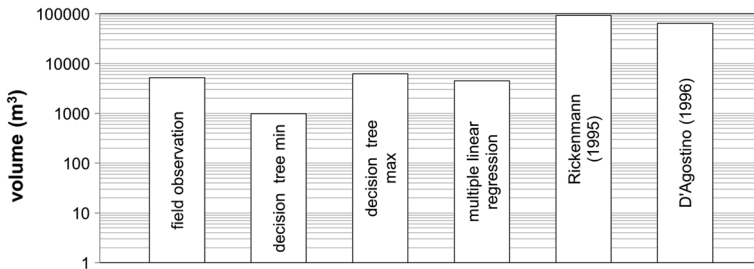


Fig. 6 Comparison of the observed total volume of the debris flow occurred in the Schipfenbach torrent with the volumes obtained by the DT (minimum and maximum values), MLR and empirical formulae

consuming field work, but they present several uncertainties, as mentioned in the review section and as observed in Fig. 6. In addition, a comparison between the DT and MLR showed several advantages of the DT: (1) it is simple, intuitive and logical, (2) it can be easily adaptable to other regions, and (3) it showed a better success than the MLR in terms of statistical parameters.

The new approach is based on both the tree obtained from our database and expert criteria. The resulting DT is presented in a qualitative form (Fig. 7) and may be adapted by introducing specific values of the different parameters according to the characteristics of the region. Several outputs of the study are included in our general approach. Firstly, sediment availability is the most influencing factor. Second, the reaches with low sediment availability (HL, CL) directly reach the leaf of the corresponding erosion rate, independently of other factors. Thirdly, for the reaches with more sediment available (ML, LL, NL), the key factors are the slope and shape. The upstream-contributing area was excluded in this final approach to simplify the DT, and because our results pointed out that it is a factor of minimum influence. The erosion classes were simplified into three classes in contrast to the four classes used in the datasets of our study.

It is important to keep in mind that the DT was developed on a dataset that includes event volumes from thousands up to a few tens of thousands of cubic metres (see Table 1). Therefore, extreme events (hundreds of thousands or even millions of cubic metres) are not

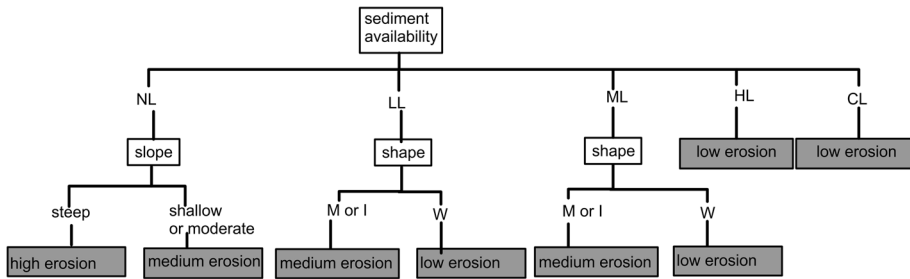


Fig. 7 General DT proposed as a learning model to estimate the erosion rate in a torrent reach

considered. Thus, results of this study are representative for medium and high-frequency debris flows that occur in the Pyrenees and Alps, but not for extreme or low-frequency events with considerably larger volumes. Last but not least, if the method will be applied to other mountainous regions, the values of both the governing factors and the erosion rates should be adapted.

6 Conclusions

The entrainment during a debris flow is a complex process. There are different methods to predict the erosion along a debris-flow trajectory and total volume of an event. While empirical equations are straightforward and useful to obtain preliminary values of debris-flow volume, detailed information on topographical data and field observations is necessary to determine the erosion rate more precisely.

The preliminary analysis of the field and topographical information collected in 110 channel reaches of 17 debris flows supported the outcomes of previous studies that there is no clear correlation between the erosion rate and pairs of governing factors. This has also been observed by other authors (Chen et al. 2005; Hungr et al. 2005), which reinforces the complexity of the entrainment process.

Learning techniques were applied in order to obtain knowledge that describes a model that is able to predict the erosion rate in a torrent reach based on several governing factors. The entrainment showed better performance in the DT J48 model than in MLR model, even if the MLR model revealed good results in the application to our test case (Schipfenbach torrent). The resulting DT revealed that the sediment availability is the most relevant factor in the erosion process, followed by reach-averaged slope and cross section shape. In this study, the sediment availability in a torrent reach was defined by five different classes according to the overall relation between bedrock and colluvium in the cross section. It must be stated that colluvium was mostly poorly consolidated and highly erosive material accumulated from older torrential and hill slope processes. These specific conditions of the material properties might have affected the importance of this factor and should be checked, if the model will be applied in different environments.

Finally, we proposed a simple prediction model for debris-flow erosion rate in channel reaches. The approach is based on both the DT obtained from our database and expert criteria. We presented the DT in a qualitative way in order to make it adaptable to other regions. It must be stated that this approach only estimates the entrainment directly related to both channel-bed erosion and local failures of channel banks neglecting large failures in torrent slopes.

In spite of the limited number of reaches in our database, the outcomes of this study improve the understanding of debris-flow entrainment. In addition, the general DT represents a useful tool to estimate the total event volume, since the determination of the volume without considering the entrainment could considerably underestimate the real volume involved in the event. Regarding a hazard assessment at catchment scale, the general DT could be applied to any torrent, after calibrating the limit values of the classes of the geomorphological factors. Moreover, the values of the erosion rates should be adapted to the values observed in each specific region, since they may be higher than the ones in this study.

Acknowledgments This research has been funded by the Spanish Ministry MINECO contract CGL2011-23300 (project DEBRIS-START). We would like to thank the Gesäuse National Park, the Aigüestortes i Estany de Sant Maurici National Park, François Xavier Marquis, Institut Geològic de Catalunya (IGC) and the WSL for their support on data acquisition. We are grateful to Christian Scheidl, Vicente Medina, Carlo Gregoretti, José Moya and the two anonymous reviewers for their constructive comments on previous versions of the manuscript and the DT and Mar Obrador for improving our English writing.

References

- Berger C, McArdell BW, Schlunegger F (2011) Sediment transfer patterns at the Illgraben catchment, Switzerland: implications for the time scales of debris flow activities. *Geomorphology* 125:421–432
- Bovis MJ, Jakob M (1999) The role of debris supply conditions in predicting debris flow activity. *Earth Surf Process Land* 24:1039–1054
- Breien H, De Blasio FV, Elverhoi A, Hoeg K (2008) Erosion and morphology of a debris flow caused by a glacial lake outburst flood, Western Norway. *Landslides* 5:271–280
- Breiman L, Friedman J, Olshen R, Stone C (1984) Classification and regression trees. Wadsworth & Brooks/Cole Advanced Books & Software, London
- Chen J, YP H, FQ W (2005) Debris flow erosion and deposition in Jiangjia Gully, Yunnan, China. *Environ Geol* 48:771–777. doi:[10.1007/s00254-005-0017-z](https://doi.org/10.1007/s00254-005-0017-z)
- Chevalier G, Medina V, Hürlimann M, Bateman A (2013) Online available. Debris-flow susceptibility analysis using fluvio-morphological parameters: application to the Central-Eastern Pyrenees. *Nat Hazards*. doi:[10.1007/s11069-013-0568-3](https://doi.org/10.1007/s11069-013-0568-3)
- Coussot P, Meunier M (1996) Recognition, classification and mechanical description of debris flows. *Earth Sci Rev* 40:209–227
- Crosta GB, Imposimato S, Roddeman D (2009) Numerical modelling of entrainment/deposition in rock and debris-avalanches. *Eng Geol* 109:135–145
- D'Agostino V (1996) Analisi quantitativa e qualitativa del trasporto solido torrentizio nei bacini montani del Trentino Orientale, 1a Sezione, Volume presentato in occasione del Convegno di Studio: I problemi dei grandi comprensori irrigui, Novara, pp 111–123
- Degetto M, Crucil G, Pimazzoni A, Masetto C, Gregoretti C (2011) An estimate of the sediments volume entrained by debris flow along Strobel and South Pezories channels at Fiames (Dolomites, Italy). In: Genevois R, Hamilton D, Prestininzi A (eds), 5th International Conference on Debris Flow Hazards. Mitigation, Mechanics, Prediction and Assessment. Casa Editrice Università La Sapienza, Padua, Italy, pp 845–855
- Denlinger RP, Iverson RM (2001) Flow of variably fluidized granular masses across three-dimensional terrain 2. Numerical predictions and experimental tests. *J Geophys Res B* 106:553–566
- Dong JJ, Lee CT, Tung YH, Liu CN, Lin KP, Lee JF (2009) The role of the sediment budget in understanding debris flow susceptibility. *Earth Surf Process Land* 34(12):1612–1624
- Egashira S, Honda N, Itoh T (2001) Experimental study on the entrainment of bed material into debris flow. *Phys Chem Earth Part C* 26(9):645–650
- ESRI (2005) ArcGIS 9: what is ArcGIS 9.1? ESRI, Redlands, CA
- Fannin RJ, Rollerson TP (1993) Debris flows: some physical characteristics and behaviour. *Can Geotech J* 30:71–81
- Fannin RJ, Wise MP (2001) An empirical-statistical model for debris flow travel distance. *Can Geotech J* 38:982–994
- Fawcett T (2006) An introduction to ROC analysis. *Pattern Recognit Lett* 27(8):861–874

- Fayyad U, Piatetsky-Saphiro G, Smyth P (1996) From data mining to knowledge discovery in databases. *AI Magazine* 17(3):37–54
- Franzi L, Bianco G (2001) A statistical method to predict debris flow deposited volumes on a debris fan. *Phys Chem Earth* 26(9):683–688
- Gabet EJ, Bookter A (2008) A morphometric analysis of gullies scoured by post-fire progressively bulked debris flows in southwest Montana, USA. *Geomorphology* 96:298–309. doi:[10.1016/j.geomorph.2007.03.016](https://doi.org/10.1016/j.geomorph.2007.03.016)
- Gartner JE, Cannon SH, Santi PM, DeWolfe VG (2008) Empirical models to predict the volumes of debris flows generated by recently burned basins in the western US. *Geomorphology* 96:339–354
- Gertsch E (2009) Geschiebelieferung alpiner Wildbachsysteme bei Grossereignissen—Ereignisanalysen und Entwicklung eines Abschätzverfahrens Universität Bern, Bern, p 204
- Guthrie RH, Hockin A, Colquhoun L, Nagy T, Evans SG, Ayles C (2009) An examination of controls on debris flow mobility: evidence from coastal British Columbia. *Geomorphology* 114(4):601–613
- Hall MA, Frank E, Holmes G, Pfahringer B, Reutmann P, Witten IH (2009) The WEKA data mining software: an update. *SIGKDD Explor* 11(1):10–18
- Hripesak G, Rothschild AS (2005) Agreement, the f-measure, and reliability in information retrieval. *J Am Med Inf As* 12:296–298
- Hungr O, Morgan GC, Kellerhals R (1984) Quantitative analysis of debris torrent hazards for design of remedial measures. *Can Geotech J* 21:663–677
- Hungr O, McDougall S, Bovis M (2005) Entrainment of material by debris flow. In: Jakob M, Hungr O (eds) *Debris-flow hazards and related phenomena*. Springer, Berlin, pp 135–158
- Hürlimann M, Rickenmann D, Graf C (2003) Field and monitoring data of debris-flow events in the Swiss Alps. *Can Geotech J* 40(1):161–175
- Hürlimann M, Abancó C, Moya J, Vilajosana I (2013) Results and experiences gathered at the Rebaixader debris-flow monitoring site. Central Pyrenees, Spain
- Iverson RM (2012) Elementary theory of bed-sediment entrainment by debris flows and avalanches. *J Geophys Res F Earth Surface* 117:F03006. doi:[10.1029/2011JF002189](https://doi.org/10.1029/2011JF002189)
- Iverson RM, Reid ME, Logan M, LaHusen RG, Godt JW, Griswold JP (2011) Positive feedback and momentum growth during debris-flow entrainment of wet bed sediment. *Nat Geosci* 4(2):116–121
- Jakob M, Bovis M, Oden M (2005) The significance of channel recharge rates for estimating debris-flow magnitude and frequency. *Earth Surf Process Landf* 30:755–766
- Kronfeller-Kraus G (1985) Quantitative estimation of torrent erosion, International Symposium on Erosion and Disaster Prevention, Tsukuba (Japan)
- Mangeny A (2011) Landslide boost from entrainment. *Nat Geosci* 4:77–78
- Mangeny A, Roche O, Hungr O, Mangold N, Faccanoni G, Lucas A (2010) Erosion and mobility in granular collapse over sloping beds. *J Geophys Res* 115(F03040). doi:[10.1029/2009JF001462](https://doi.org/10.1029/2009JF001462)
- Marchi L, D'Agostino V (2004) Estimation of debris-flow magnitude in the Eastern Italian Alps. *Earth Surf Process Landf* 29(2):207–220
- Marchi L, Cavalli M, Sangati M, Borga M (2009) Hydrometeorological controls and erosive response of an extreme alpine debris flow. *Hydrol Process* 23:2714–2727
- Marquis FX (2006) Torrents des Glariers et du Pessot- lave torrentielle et inondation du 22.07.2006: description et analyse de l'événement, Commune de Collombey-Muraz, Monthey
- Marquis FX (2008) Lave torrentielle du 29.06.08-Description et analyse de l'événement (Torrent Sec), Communes de Collonges et de Lavey-Morcles, Monthey
- McDougall S, Hungr O (2004) A model for the analysis of rapid landslide motion across three-dimensional terrain. *Can Geotech J* 41:1084–1097
- Medina V, Hürlimann M, Bateman A (2008) Application of FLATModel, a 2D finite volume code, to debris flows in the northeastern part of the Iberian Peninsula. *Landslides* 5:127–142
- Muñoz A (1992) Evolution of a continental collision belt: ECORS-Pyrenees crustal balanced cross-section. In: McClay KR (ed) *Thrust tectonics*. Chapman & Hall, London, pp 235–246
- Oller P, Pinyol J (2009) Nota de la sortida de camp a la barrera flexible d'anells a Erill la Vall i als corrents d'arrossegalls a la vall de Sant Nicolau al Parc Nacional d'Aigüestortes i Estany de Sant Maurici, Institut Geològic de Catalunya
- Papa M, Egashira S, Itoh T (2004) Critical conditions of bed sediment entrainment due to debris flow. *Nat Hazards Earth Sci.* 4(3):469–474
- Pierson TC, Scott KM (1985) Downstream dilution of a Lahar: transition from debris flow to hyperconcentrated streamflow. *Water Resour Res* 21(10):1511–1524
- Pinyol J (2008) Nota tècnica sobre la visita al barranc de Portainé i al barranc des Caners els dies 1 i 2 d'octubre 2008 en motiu de la torrentada ocorreguda la matinada del dia 12 de setembre de 2008. Institut Geològic de Catalunya

- Rickenmann D (1995) Beurteilung von Murgängen. *Schweiz Ingenieur und Architekt* 113(48):1104–1108
- Rickenmann D, Zimmermann M (1993) The 1987 debris flows in Switzerland: documentation and analysis. *Geomorphology* 8:175–189
- Rickenmann D, Weber D, Stepanov B (2003) Erosion by debris flows in field and laboratory experiments. In: Rickenmann D, Chen C (eds) 3rd international conference on debris-flow hazards mitigation. Millpress, Davos, pp 883–894
- Scheidl C, Rickenmann D, Chiari M (2008) The use of airborne LIDAR data for the analysis of debris flow events in Switzerland. *Nat Hazards Earth Syst Sci* 8:1113–1127
- Spreafico M, Lehmann C, Naef O (1999) Recommandations concernant l'estimation de la charge sédimentaire dans les torrents. Groupe de travail pour l'hydrologie opérationnelle, Berne
- Takei A (1984) Interdependence of sediment budget between individual torrents and river-system. *Interpraevent, Villach, Austria*, pp 35–48
- Theule J, Liébault F, Loye A, Laigle D, Jaboyedoff M (2012) Sediment budget monitoring of debris-flow and bedload transport in the Manival Torrent, SE France. *Nat Hazards Earth Syst Sci* 12:731–749
- VanDine DF (1985) Debris flows and debris torrents in the southern Canadian Cordillera. *Can Geotech J* 22:44–68
- Wan S, Chiang Lei T (2009) A knowledge-based decision support system to analyze the debris-flow problems at Chen-Yu-Lan River, Taiwan. *Knowledge-Based Syst* 22:580–588
- Witten IH, Frank E, Hall MA (2011) *Data mining: practical machine learning tools and techniques*, 3rd edn. Morgan Kaufmann, Burlington
- Zeller J (1985) Feststoffmessung in kleinen Gebirgseinzugsgebieten. *Wasser Energie Luff* 77(7/8):246–251